

GEO-ELECTRICAL INVESTIGATION OF GROUNDWATER POTENTIAL ZONES OF GASSOL L.G.A USING ELECTRICAL RESISTIVITY METHOD

Moshud K. Musa.,^{1*} Rimamsiwe Alfred¹, Achimugu Augustina¹, Mohammed F. Isa²,
Abubakar K. Orume¹, Sa'adu B. Abubakar³

^{1*}Department of Pure and Applied Physics, Federal University Wukari,
Taraba State.

²Department of Physics, Modibbo Adama University Yola, Adamawa State.

³Federal university Wukari.

* **Correspondence:** Moshud K. Musa

*The authors declare
that no funding was
received for this work.*



Received: 26-December-2025

Accepted: 22-February-2026

Published: 25-February-2026

Copyright © 2026, Authors retain copyright. Licensed under the Creative Commons Attribution 4.0 International License (CC BY 4.0), which permits unrestricted use, distribution, and reproduction in any medium, provided the original work is properly cited.
<https://creativecommons.org/licenses/by/4.0/> (CC BY 4.0 deed)

This article is published in the **MSI Journal of Multidisciplinary Research (MSIJMR)** ISSN 3049-0669 (Online)

The journal is managed and published by MSI Publishers.

Volume: 3, Issue: 2 (February-2026)

ABSTRACT: Geophysical investigation of groundwater potential of Gassol L.G.A. Taraba state, Nigeria was carried out using electrical resistivity method ERM with the aim of evaluating the seasonal variation/change in boreholes water of the study area. A total of twenty five (25) vertical electrical sounding VES were conducted with maximum electrode spacing of 200 m for deeper aquifer depth investigation due to the hydrogeology of the area. The primary geoelectrical field data (apparent resistivity and strata thickness) were acquired using ABEM SAS 1000 Terameter and interpreted using Interpex software. The result revealed five (5) subsurface geoelectrical layers: topsoil, sandy-clay, clayed-sand, laterite, sandstone (aquifer) and consolidated sandstone. The resistivity values of the VES points were mostly low in the sedimentary terrain except in VES 16, 17, 18, 19, 20, 22 and 25. The resistivity and thickness values range from 0.186 Ω m to 9536.500 Ω m and 0.208 m – 80.760 m. Thickness of the aquifer stratum only does not determine the groundwater potential rather the porosity and permeability of this thick layer. Depth to aquifer range from 3.300 m to 93.700 m while the resistivity values of

the aquifer ranged from 1.320 to 6463.500 Ωm with an unconfined aquifer presence in VES 2, 4, 9, 10, 11, 12, 14, 16, 22 and 25 where the resistivity of the strata below the unconfined aquifers range from 0.186 Ωm to 86.390 Ωm . The seasonal change/variation in the groundwater potential of the study area is due to the depth of the unconfined aquifer used for drilling instead of the confined aquifer depth. Hydrogeological study and Proper geoelectrical resistivity survey with wide electrodes spacing (> 200 m) for deeper aquifer depth information should be conducted so to prevent seasonal variation/change of the groundwater potential from boreholes.

Keywords: *sedimentary terrain, geoelectric resistivity parameters, porosity, permeability, groundwater potential, unconfined aquifer, aquifer depth*

Introduction

Groundwater is the water contained beneath the earth surface in rocks and soils. It is the water that accumulates underground in aquifers. Groundwater constitutes 97 per cent of global freshwater and is an important source of drinking-water in many regions of the world. In many parts of the world groundwater sources are the single most important supply for the production of drinking-water, particularly in areas with limited or polluted surface water sources. For many communities it may be the only economically viable option. Groundwater often required little or no treatment to be suitable for drinking whereas surface waters generally need to be treated, often extensively (Oliver *et al.*, 2006). Aquifer is the geological formation which serves as reservoir for groundwater in sedimentary and basement terrain. Groundwater occurrence and accumulation in the aquifer depends on the degree and thickness of the weathering; the degree and nature of fracturing of the rock; and the hydrogeological continuity (permeability) of the weathered or fractured zones (Akinwumiju *et al.*, 2016).

Successful geophysical exploration of groundwater bearing zones from the earth surface and exploitation the groundwater through the construction of boreholes and hand-dug wells construction required a geophysicist (Joel *et al.*, 2020). The failure of boreholes and hand-dug wells as well as increased contamination of groundwater sources (aquifer) is due to lack of requisite groundwater exploration and exploitation

knowledge and skills which led to the haphazard means of groundwater exploitation (Talabi, 2018; Ajayi and Abegurin 1994; Cobbina *et al.*, 2014). Groundwater potential of the sedimentary rocks is higher than that of basement Complex rocks used for domestic, industrial and agricultural purposes. The groundwater is weakly acidic with small amount of TDS, hence falls within the fresh water category. The groundwater is not potable but could serve domestic and general purposes (Owolabi *et al.*, 2022). For suitable groundwater extraction due to the existence of unconfined aquifer future boreholes drillers should target only confined aquifer for successful groundwater exploration in sedimentary and basement terrain (Mark *et al.*, 2000).

Groundwater sources are largely reliable resources for use as drinking-water in most parts of Nigeria, as seen in Gassol Local Government Area of Taraba state. Commercial activities experienced has contributed to the population soar of this area, consequently high demand for potable water is on rise. Groundwater been the only source of potable water has led to increase in the boreholes drilling for available and quality groundwater supplied. Health and financial factors associated to groundwater exploration and exploitation has necessitate the geo-electrical resistivity investigation of groundwater potential of Gassol L.G.A with VES electrode spacing of 200 m in order to delineate the depth to aquifer (confined) and its lateral extent for positive hydrogeological result which prevents possible seasoning variation/change in the borehole water supplied.

DESCRIPTION OF THE STUDY AREA

The study was conducted in Gassol Local Government Area of Taraba state; it is located between latitude 7° 32' to 8° 40' N and longitude 10° 25' to 11° 15' E. The local government has a landmass of 5,982 *Km*² and a population of 244,749 according to the National Population Census (2006) and is one of the most populous local government areas in the State. It is 75 km away from Jalingo the State capital. About 80 %, of its population are crop farmers while others are cattle breeders and fishermen. The area has tropical continental type of climate characterized by well-marked wet and dry season. The rainy season usually starts around May and ends in October, while the dry season begins in November and ends in April. The annual rainfall is 859 ± 25 mm with onset and cessation on 2nd May (± 3 days) and 4th

November (± 4 days), of every year respectively. The length of the growing season is 187 (± 15 days). There is direct correlation between rainfall and relative humidity; hence, the relative humidity during the wet season ranges between 60 and 70 %, while the relative humidity during the dry season ranges between 35 and 45 %. In general, the temperature is high throughout the year; hence it is favorable for cultivation of crops in the area. The average monthly temperature ranges between 26 and 32 °C (Adeyolanu *et al.*, 2020).

The area falls within the Middle Benue Basin with River Benue as the principal drainage system. The northern border of Gassol watershed is the Benue River while Taraba river flows north through the Gassol to its confluence with the Benue River. River Taraba is the major drainage of Gassol watershed with other rivers discharging into it. The floodplains of the Taraba River constitute the major agricultural land in Gassol. The areas are irrigable low-lying floodplains characterized by low slope (0 - 3 %). The flat nature of the topography contributes to the challenge of flooding often face by farmers in the area. The plains are currently being cultivated; however, the level of irrigation practices is still low. The water management in the watershed entails use of surface water conservation practices including basin and construction of bunds as water conservation strategy. This is very effective and should be encouraged. Water lifting from the rivers is also being practiced using small petrol pumps.

Commercial activities experienced in Gassol has contributed to the population soar of this area, consequently high demand of potable water is on rise. Groundwater been the only source of potable water has led to increase in the boreholes drilling for available and quality groundwater supplied. Health and financial factors associated to the groundwater exploration and exploitation has necessitate the geo-electrical resistivity investigation of groundwater potential of Gassol LGA with VES electrode spacing of 200 m in order to delineate the depth to aquifer (confined) and its lateral extent for positive drilling result which prevents possible seasoning variation/change in the borehole water supplied.

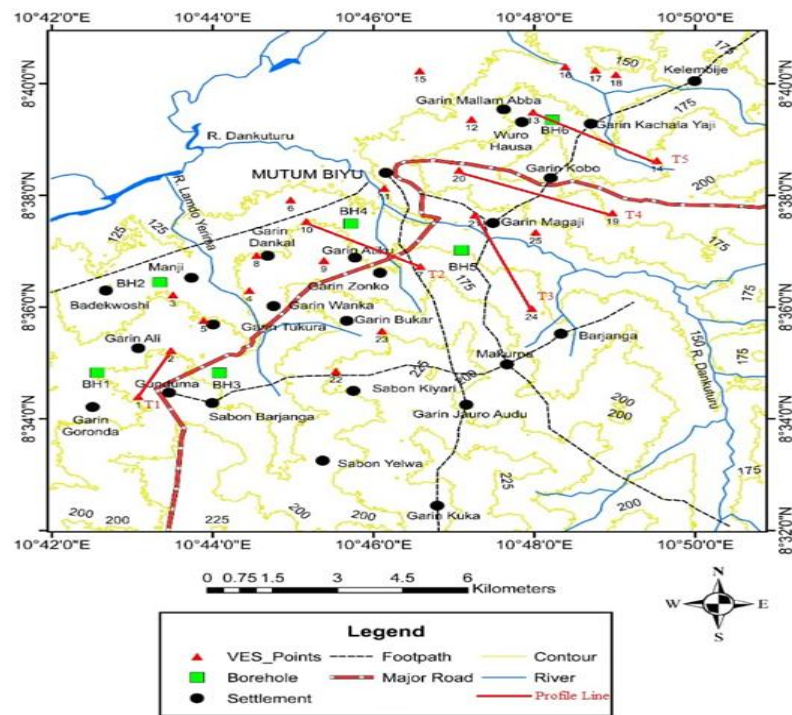


Figure 1: Map of the Study Area with VES points

METHODOLOGY

The study therefore adopted the electrical resistivity survey method (ERM) which is a geophysical survey technique that has proven to be an effective and a reliable tool in locating viable aquifers for continuous and regular water supply (Adeniji *et al.*, 2013), this method has the advantage of non-destructive effect on the environment, cost-effective, rapid and quick survey time and less ambiguity interpretations of the results when compared to other geophysical survey methods. The most popular configuration in vertical electrical sounding (VES) is the conventional Schlumberger array, which has a symmetrical layout with electrodes spread on either side of the array spread (Oladunjoye and Jekayinfa 2015; Olorunfemi *et al.*, 2005). Geo-electrical resistivity methods are based on the effective response of the earth to the flow of subsurface electrical current. The method involves passing electrical current into the ground by means of two current electrodes $AB/2$ and two potential electrodes $MN/2$ used to record the resultant potential difference between them, thereby resulting in the measurement of electrical impedance (Egbai, 2013). The

fundamental physical law used in resistivity surveys is Ohm's law that governs the flow of current in the ground.

The electrical resistivity of a rock formation limits the amount of current passing through the formation when an electrical potential is applied. If a material of resistance R has a cross-sectional area A and a length L , then its resistivity can be expressed

$$\rho = \frac{RA}{L}$$

ρ is the resistivity measured in Ohms-metres, R is resistance in Ohms, cross sectional area A in metres-squared and length L in metres.

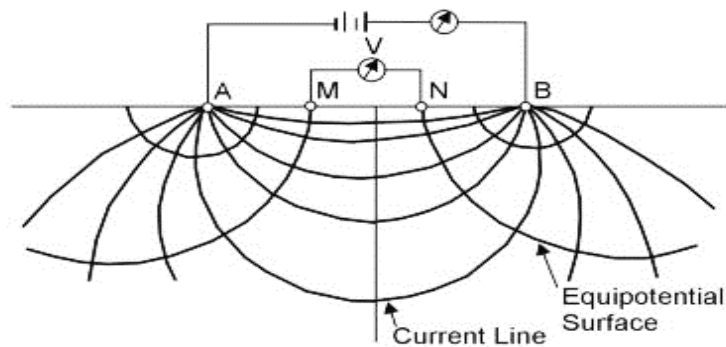


Figure 2: The potential distribution caused by a pair of current electrodes

DATA PROCESSING

Interpex IX1D geoelectrical computer software was adopted to process the georesistivity field data obtained with a maximum electrodes spacing of 200 m in the study area. The field apparent resistivity with its corresponding $AB/2$ (m) was inputted into the software for additional modelling and iteration. The physical result obtained from the software modelling includes; true resistivity of each subsurface layer with corresponding thickness and depth.

DATA INTERPRETATION

Geoelectrical resistivity field curves graphically showed the relationship between apparent resistivity (ρ_a) and the current electrode $AB/2$ spacing. Hydrogeological

interpretation of VES data involves two methods: The qualitative data interpretation which involves the examination of resistivity field curve types (A, H, K, and Q) and their quality. Apparent resistivity profiles were constructed enabling a visual and qualitative assessment of the successive geo-electrical layers. This preliminary evaluation helped in understanding the detected subsurface features.

The second method involves quantitative data interpretation and this involves the determination of the resistivities and thicknesses of the different subsurface strata. Geo-electrical sections were constructed and these sections were then converted into geological sections by integrating lithological information from existing wells and other available sources. Lacked of such geological data could present challenges specially dealing with field curves associated with more than three layers (El-Osta *et al.*, 2021).

RESULTS AND DISCUSSIONS

Twenty-five (25) VES points were covered along the NE-SW direction in different wards of the study area. Representative inverse model curves for the geoelectric resistivity parameters obtained from the computer iteration were shown in figure 3 - 9 which include KHK, AKQ, A, HAK, K, KH, Q, HK, QHK, AHK, HKH, QH, HKQ, AA, and H curve types, were KHK consists 4 % of the curves, AKQ 4 %, A 4 %, HAK 8 %, K 8 %, KH 12 %, Q 4 %, HK 28 %, QHK 4 %, AHK 4 %, HKH 4 %, QH 4 %, HKQ 4 %, AA 4 %, and H 4 % of the total curve types respectively. In general, geoelectric layers were delineated from the sounding curves, the low resistivity at the water bearing layers and the layers underlying the aquifer at some VES points observed signifies the presence of unconfined aquifer underlain by an aquitard (low permeable layer) formation and the high thickness of the aquifer layers shows the high groundwater potential level of the area.

Vertical electrical sounding (VES) conducted in different locations of the study area were plotted and smoothened with IX1D software. The results of smoothened data were interpreted and discussed.

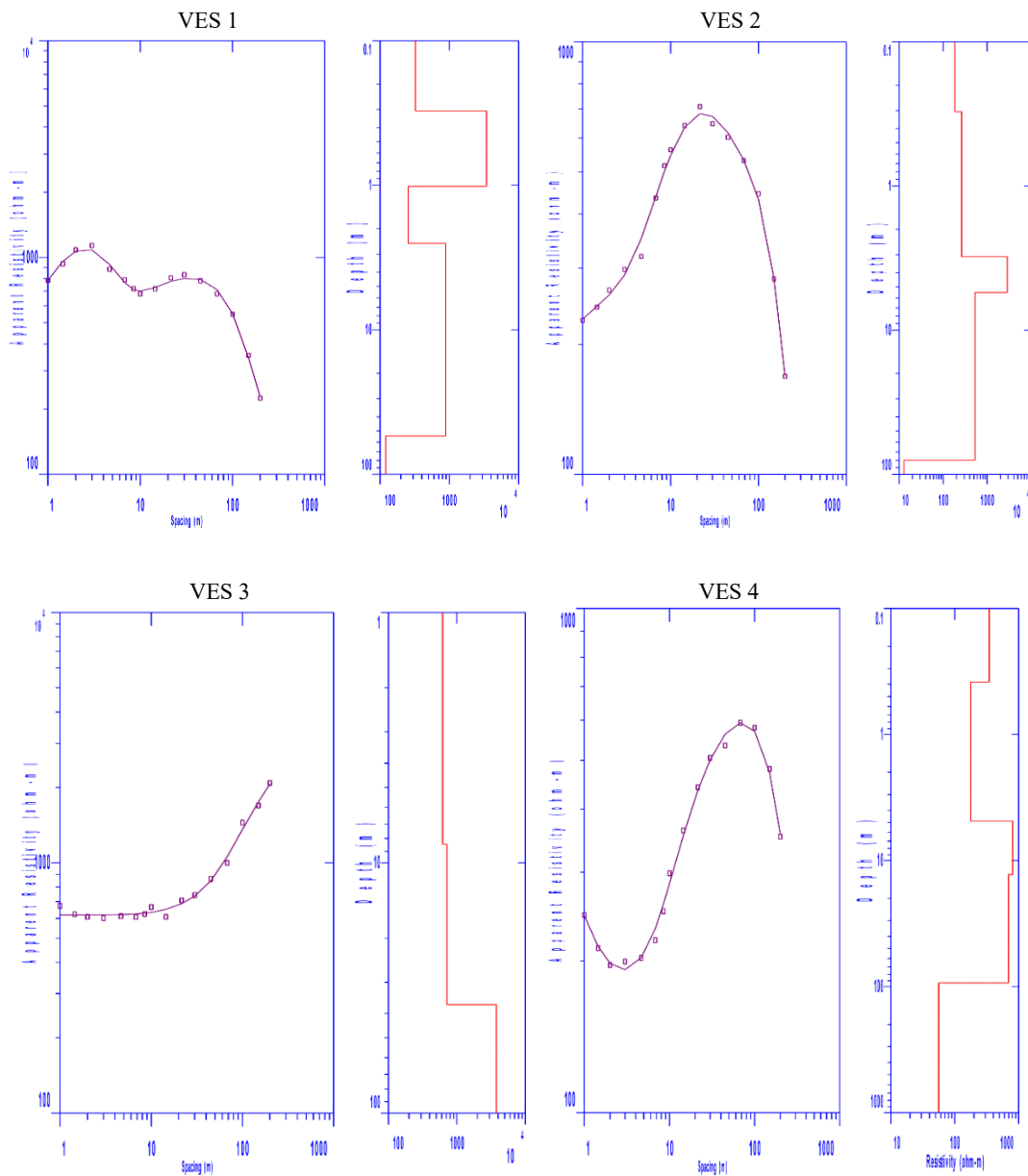


Figure 4: Curve types of VES 1, 2, 3 and VES 4

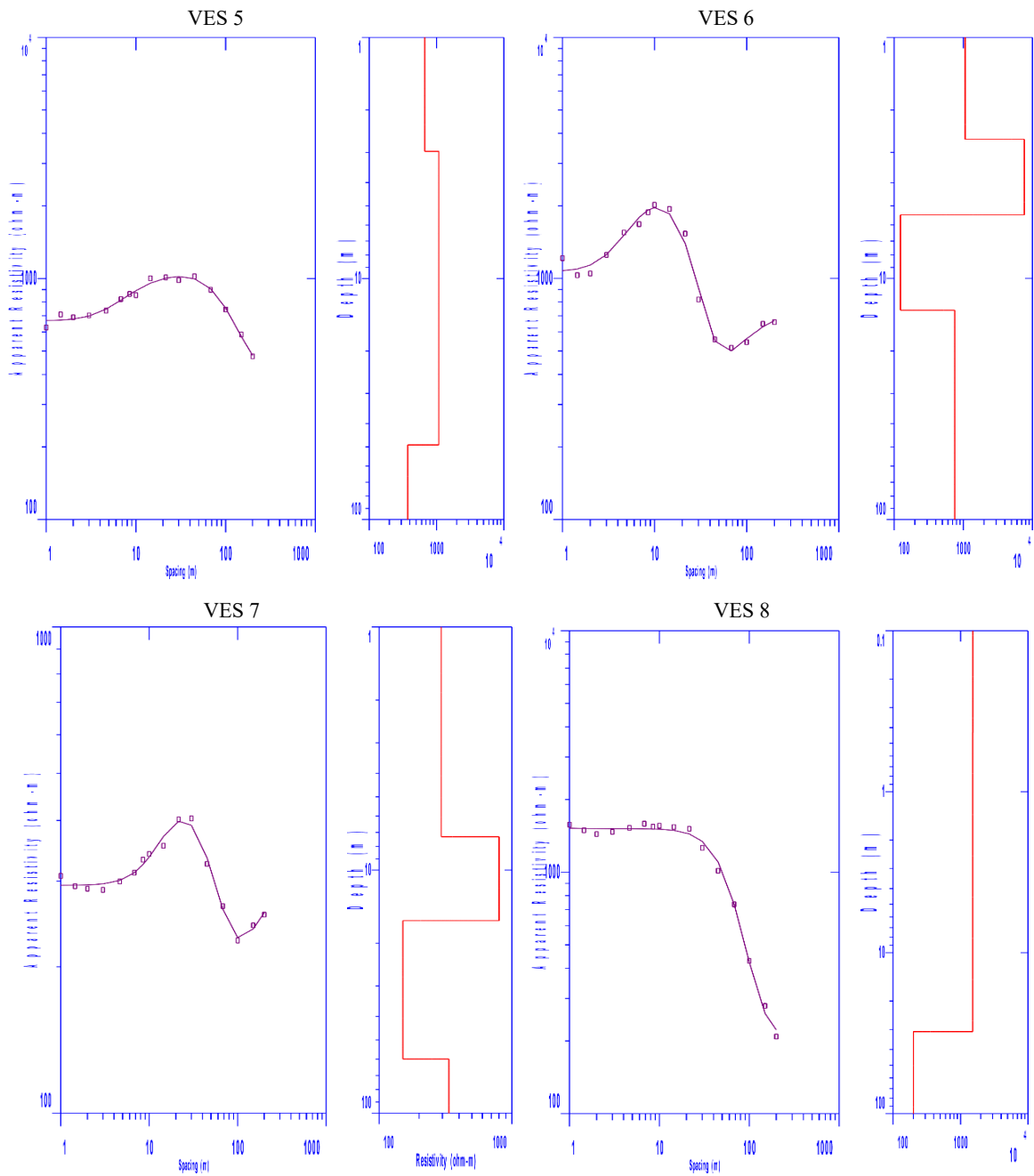


Figure 5: Curve types of VES 5, 6, 7, and VES 8

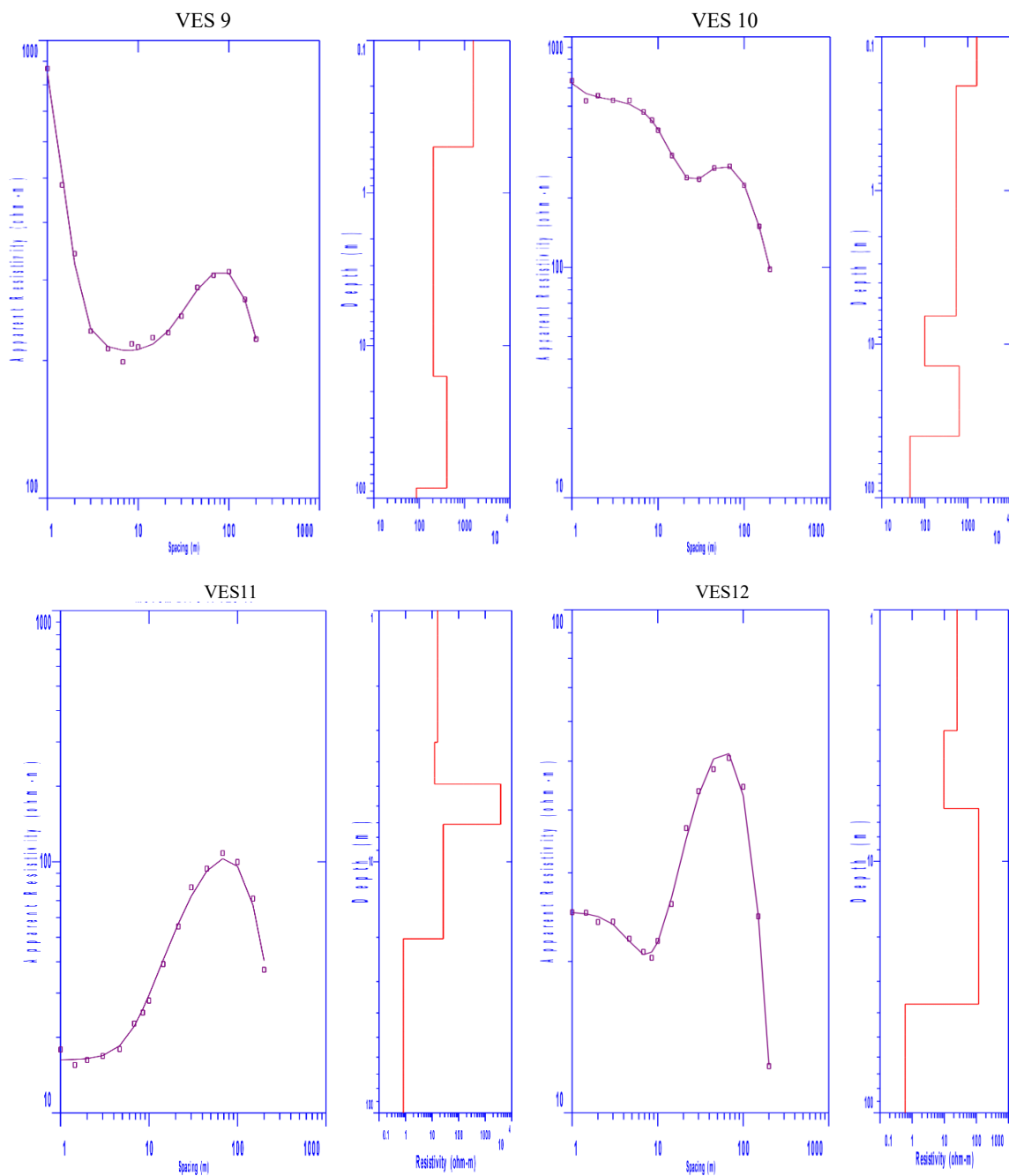


Figure 6: Curve types of VES 9, 10, 11, and VES 12

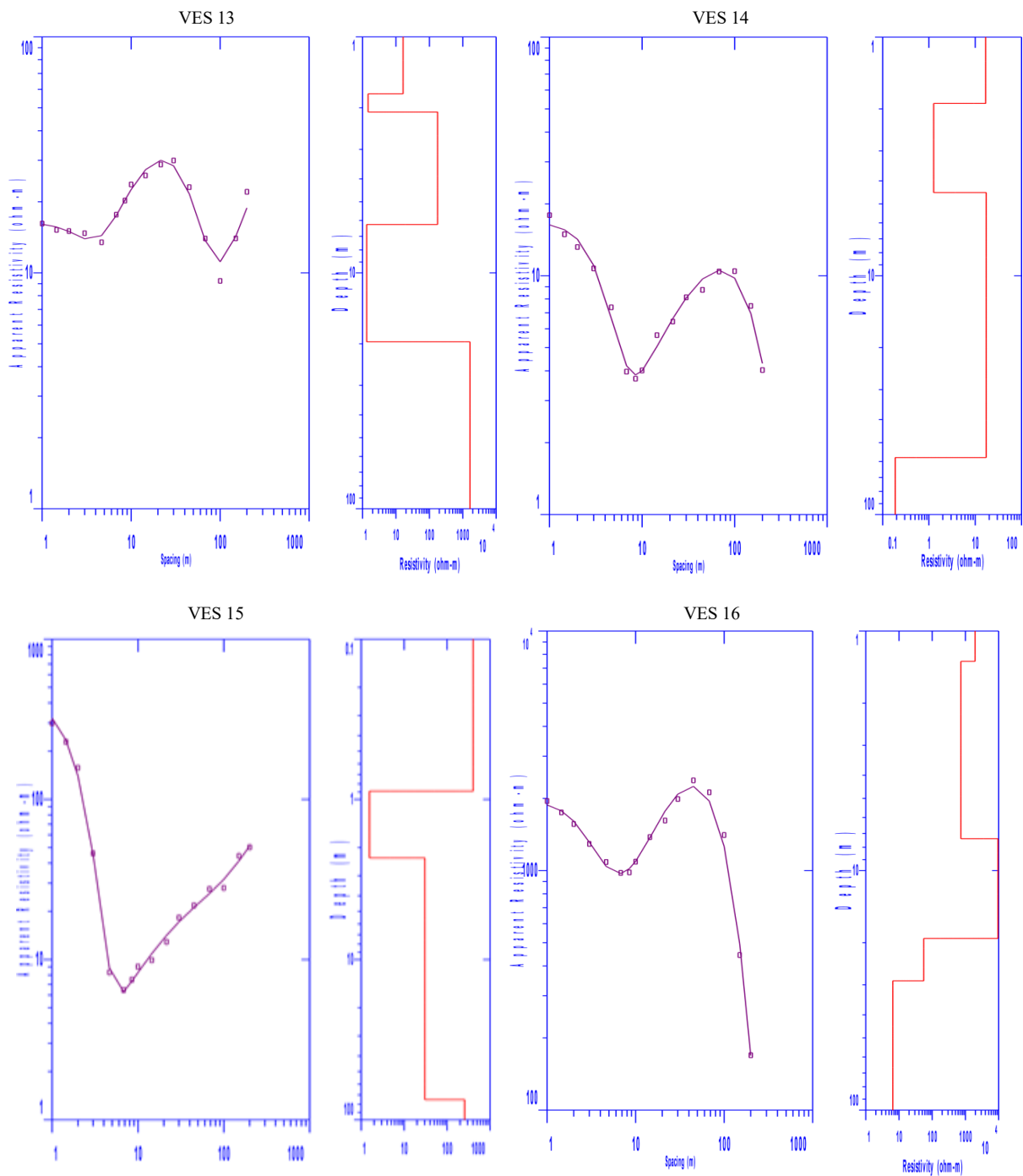


Figure 7: Curve types of VES 13, 14, 15, and VES 16

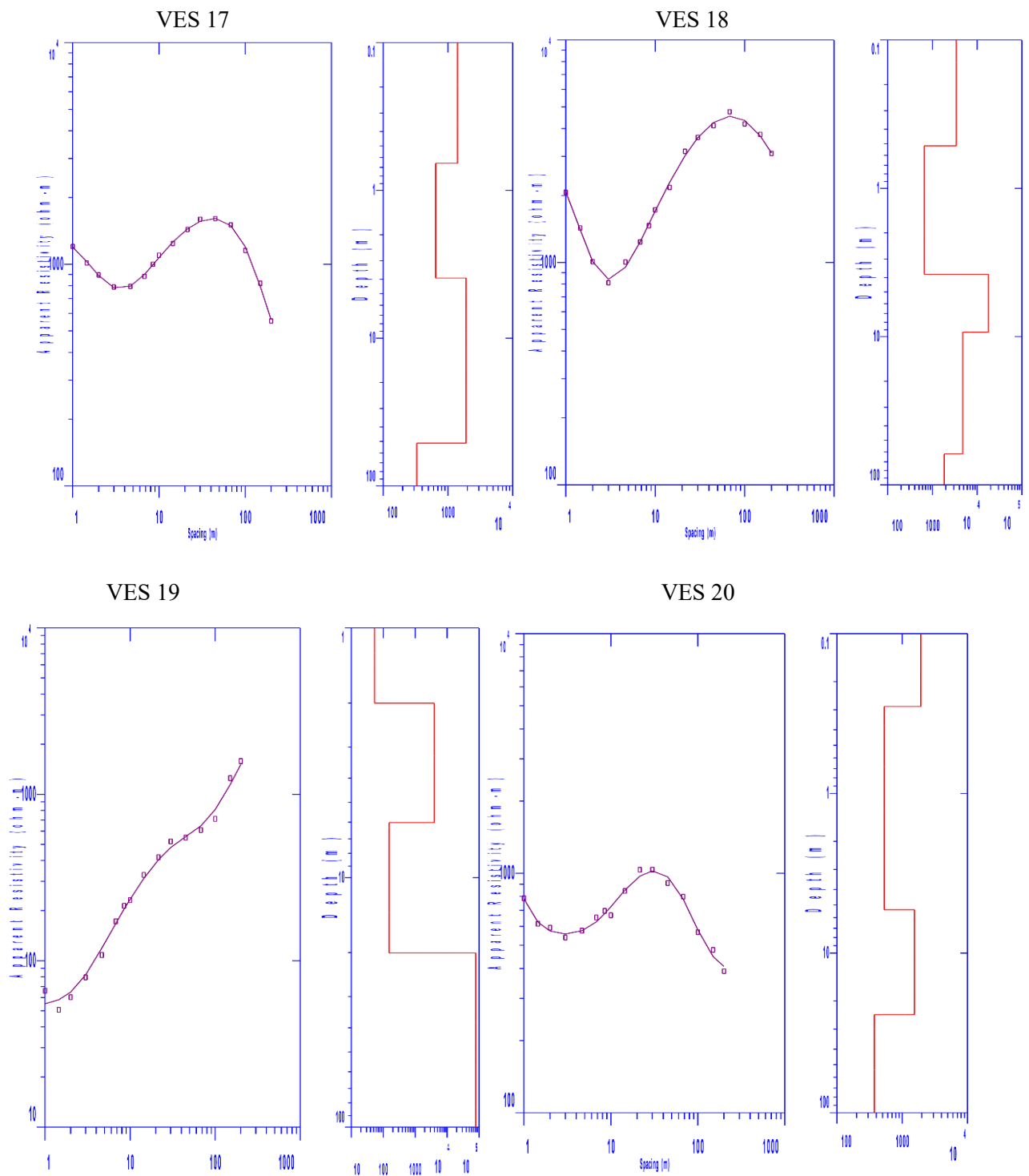


Figure 8: Curve types of VES 17, 18, 19, and VES 20

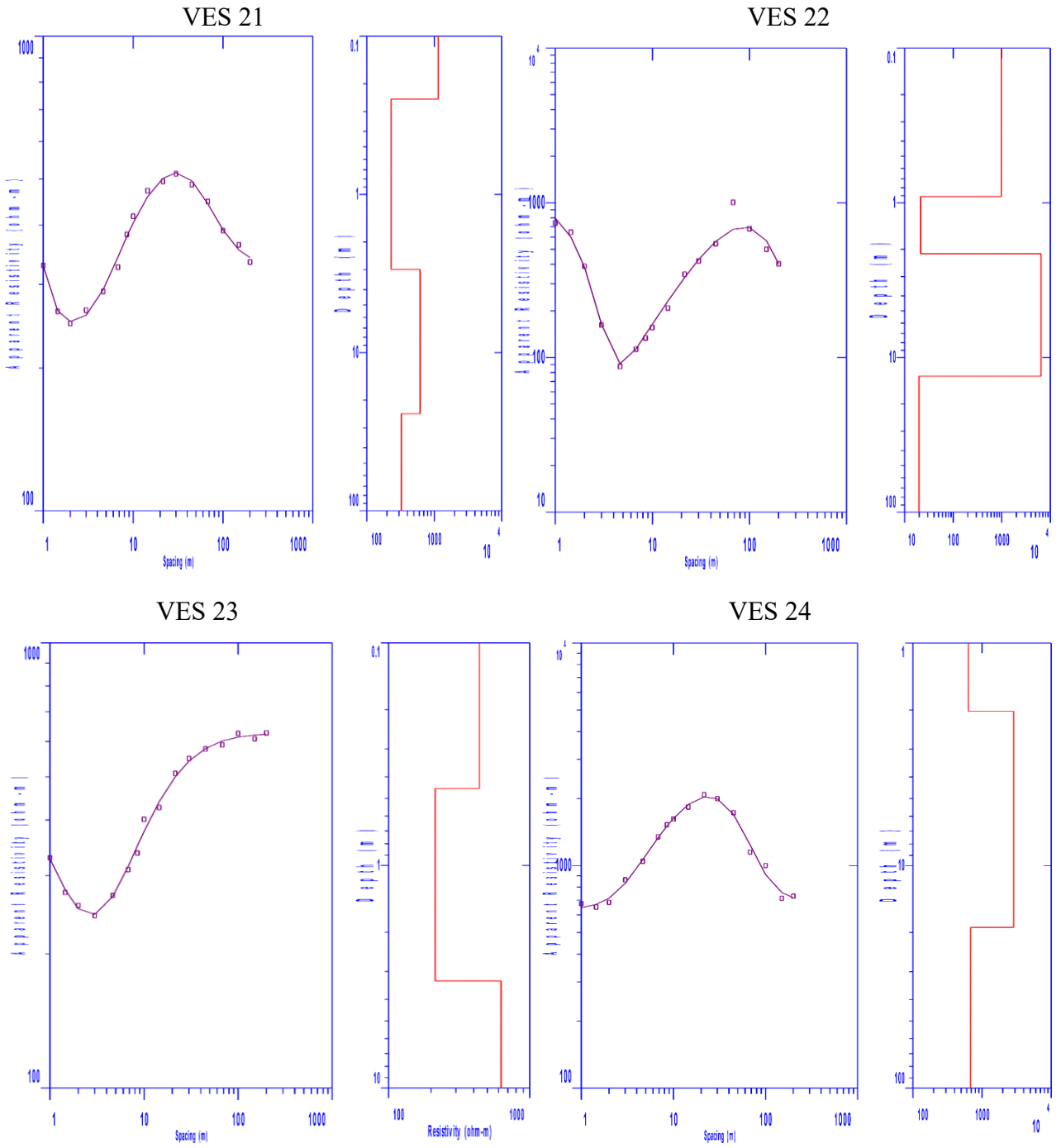


Figure 9: Curves types of VES 21, 22, 23, and VES 24

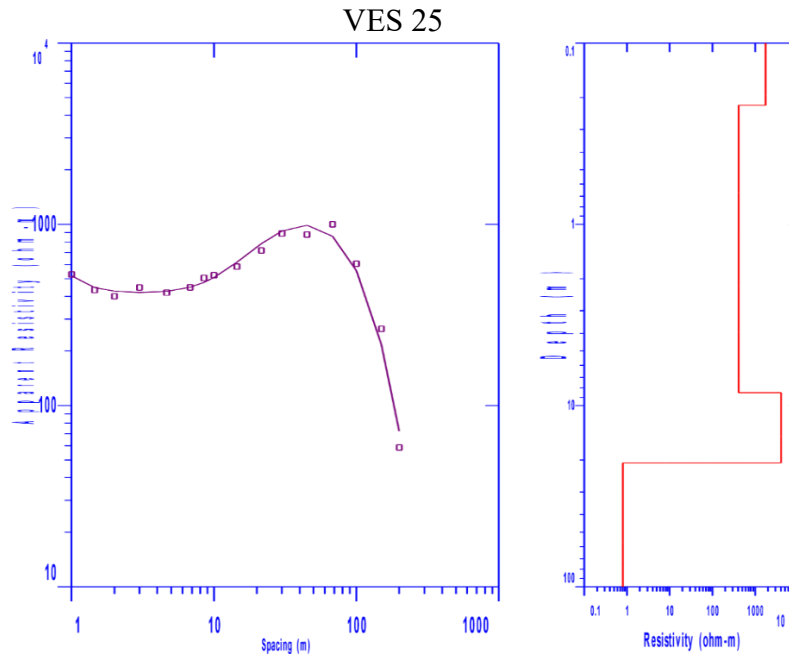


Figure 10: Curve type of VES 25

Table 1: Summary of the VES Interpretation Results

VES NO.	Curve Type	No. of Layers	Resistivity Value (Ω -m)	Thickness (m)	Depth(m)	Inferred Lithology
1	KHK	1	324.7	0.305	0.305	Topsoil
		2	3440.3	0.711	1.01	Laterite
		3	254.9	1.5	2.52	Sandy-clay
		4	883.5	51.77	54.3	Sandstone (aquifer)
		5	120.5	—	—	Wet-Sandstone
2	AKQ	1	184.2	0.304	0.304	Topsoil
		2	261.6	2.78	3.09	Sandy-clay
		3	2873	2.38	5.47	Laterite
		4	531.1	74.17	79.65	Sandstone (unconfined aquifer)
		5	12.71	—	—	Clay
3	A	1	619.3	8.42	8.42	Topsoil
		2	716.7	28.41	36.83	Sandstone (aquifer)
		3	3785.2	—	—	Consolidated-Sandstone
4	HAK	1	345.6	0.383	0.383	Topsoil
		2	177.9	4.48	4.87	Clayed-sand
		3	808.2	8.07	12.94	Sandy-clay

		4	688.9	80.76	93.7	Wet-Sandstone (unconfined aquifer)
		5	56.03	—	—	Clay
5	K	1	668.2	2.97	2.97	Topsoil
		2	1083.6	46.08	49.05	Sandstone (aquifer)
		3	373.4	—	—	Wet- Sandstone
6	KH	1	1065.8	2.64	2.64	Topsoil
		2	7659.5	2.8	5.44	Laterite
		3	123.6	8.09	13.54	Wet-Sandstone (aquifer)
		4	753.5	—	—	Sandstone
7	KH	1	294.2	7.29	7.29	Topsoil
		2	800.5	8.86	16.15	Sandy-clay
		3	150.8	43.71	59.87	Wet-Sandstone (aquifer)
		4	335.9	—	—	Sandstone
8	Q	1	1526.6	0.427	0.427	Topsoil
		2	1515.3	30.52	30.95	Sandstone (aquifer)
		3	200.2	—	—	Wet-Sandstone
9	HK	1	1567.2	0.498	0.498	Topsoil
		2	205.6	15.38	15.88	Clayed-sand
		3	405.5	69.95	85.83	Sandstone (unconfined aquifer)
		4	86.39	—	—	Clay
10	QHK	1	1607.8	0.208	0.208	Topsoil
		2	532.6	6.33	6.54	Sandy-clay
		3	99.54	7.33	13.88	Clay
		4	625.8	25.77	39.65	Sandstone (unconfined aquifer)
		5	45.17	—	—	Clay
11	AHK	1	16.25	3.34	3.34	Topsoil
		2	12.47	1.55	4.9	Clay
		3	3842.5	2.19	7.09	Laterite
		4	26.52	13.16	20.26	Clayed-sand (unconfined aquifer)
		5	0.824	—	—	Moist-Clay
12	KH	1	25.08	3.02	3.02	Topsoil
		2	9.74	3.14	6.16	Clay
		3	118.2	30.79	36.96	Sandstone (unconfined aquifer)

		4	0.606	—	—	Moist-Clay
13	HKH	1	16.36	1.74	1.74	Topsoil
		2	1.45	0.337	2.08	Clay
		3	176.4	4.15	6.23	Sandy-clay
		4	1.32	13.38	19.62	Moist-Clay (unconfined aquifer)
		5	1655.2	—	—	Sandstone
14	HK	1	16.76	1.89	1.89	Topsoil
		2	1.26	2.58	4.47	Clay
		3	17.25	53.2	57.68	Clayed sand (unconfined aquifer)
		4	0.186	—	—	Moist-Clay
15	QH	1	404	0.887	0.887	Topsoil
		2	1.55	1.43	2.31	Clay
		3	30.22	72.53	74.85	Clayed-sand (unconfined aquifer)
		4	256	—	—	Sandstone
16	HKQ	1	1951.1	1.33	1.33	Topsoil
		2	734.4	6.02	7.36	Sandy-Clay
		3	9536.5	11.84	19.2	Laterite
		4	55.82	9.65	28.86	Clayed-sand (unconfined aquifer)
		5	6.51	—	—	Clay
17	HK	1	1408.2	0.656	0.656	Topsoil
		2	648.4	3.26	3.91	Sandy-clay
		3	1915.8	47.53	51.45	Sandstone (aquifer)
		4	331.1	—	—	Wet-Sandstone
18	HAK	1	3419.5	0.517	0.517	Topsoil
		2	656	3.28	3.8	Sandy-clay
		3	17858.9	5.54	9.34	Laterite
		4	4762.2	52.51	61.85	Sandstone (aquifer)
		5	1838.7	—	—	Sandstone
19	AA	1	53.33	2	2	Topsoil
		2	3963.9	4.02	6.02	Laterite
		3	153.1	14.03	20.05	Wet-Sandstone (aquifer)
		4	79095.2	—	—	Consolidated-Sandstone
20	HK	1	1933.9	0.286	0.286	Topsoil
		2	530.9	5.07	5.35	Sandy-clay

		3	1543.6	18.97	24.33	Sandstone (aquifer)
		4	374	—	—	Wet-Sandstone
21	HK	1	1148.4	0.249	0.249	Topsoil
		2	229.1	2.72	2.97	Sandy-clay
		3	617.4	21.38	24.36	Sandstone (aquifer)
		4	326.4	—	—	Wet-Sandstone
22	HK	1	976.1	0.911	0.911	Topsoil
		2	21.24	1.22	2.13	Clay
		3	6463.5	11.08	13.22	Sandstone (unconfined aquifer)
		4	19.71	—	—	Clay
23	H	1	440.3	0.451	0.451	Topsoil
		2	213.6	2.85	3.3	Wet-Sandstone (aquifer)
		3	626.3	—	—	Sandstone
24	K	1	634.3	2.02	2.02	Topsoil
		2	2878.8	16.94	18.97	Sandstone (aquifer)
		3	682.3	—	—	Wet-Sandstone
25	HK	1	1764.3	0.22	0.22	Topsoil
		2	410	8.28	8.5	Sandy-clay
		3	4037.3	12.19	20.69	Sandstone (unconfined aquifer)
		4	0.807	—	—	Moist-Clay

DISCUSSIONS

VES 1, 2, 3, 4 and 5 conducted in the study area were KHK, AKQ, A, HAK, and K curve types (see figure 4-5) and Table 1 revealed a topsoil (sandy-clay) layer of thickness and resistivity values ranging from 0.304 - 8.420 m and 184.200 - 668.200 Ω m respectively. The topsoil layer was followed by more resistive layer as exhibited by VES 1, 2, 3, and 5 except VES 4. The second layer in VES 3 and 5 with thickness and resistivity values ranging from 28.410 - 46.080 m and 716.700 - 1083.600 Ω m respectively was identified as the aquifer layer and was interpreted to be sandstone while the fourth layer in VES 1, 2, and 4 was characterized as the aquifer unit with thickness and resistivity values from 51.770-80.760 m and 531.100-883.500 Ω m. The thickness of the reservoir layer (aquifer) of VES 1, 2, 4 and 5 conducted

revealed that the groundwater potential of the sounding points was high except VES 3 which had low aquifer thickness with shallow depth.

VES locations 6, 7, 8, 9 and 10 conducted were observed to be KH, KH, Q, HK, and QHK curve types (figure 5-6) which also exhibited different numbers of subsurface layers with resistivity and thickness values ranging from 294.200 - 1607.800 Ωm and 0.208 - 7.290 m for the topsoil (sandy-clay) layer and the stratum was underlain by a layer of lower resistivity except in VES 6 and 7. The second layer of VES 8 with resistivity and thickness values of 1515.300 Ωm and 30.520 m respectively is the reservoir unit of the VES station and was identified as sandstone. Aquifer zone of VES 6, 7, and 9 were also identified to be the third geoelectric unit characterized by resistivity and thickness values of 123.600 - 405.500 Ωm and 8.090 - 69.950 m while VES 10 was characterized by five layers, the aquiferous unit was the fourth subsurface stratum which contained an appreciable groundwater potential. Sandstone was also the aquifer layer of VES 6, 7, 8, 9, and VES 10 of this area and the groundwater potential level is also high.

VES 11, 12, 13, 14 and 15 carried out, revealed a five-earth layered in VES 11 and 13 and four subsurface layers in VES 12, 14, and 15 (see figure 6 - 7). The topsoil layer with thickness and resistivity values ranging from 0.887 - 3.340 m and 16.250 - 404.000 Ωm and was followed by a low resistive layer of resistivity and thickness values ranging from 1.260 - 12.470 Ωm and 0.337 - 3.140 m respectively and this layer was inferred as clay. The second layer was underlain by an aquiferous layer as seen in VES 12, 14 and 15 with a very low resistivity and thickness values ranging from 17.250 - 118.200 Ωm and 30.790 - 72.530 m. The aquifer unit of VES 11 and 13 were the fourth earth layer of resistivity and thickness value of 1.320 - 26.520 Ωm and 13.160 - 13.380 m. A very low resistivity value of the aquifer unit and the underlain unit in the study area showed the existence of an unconfined aquifer.

VES 16, 17, 18, 19 and 20 conducted, shown in figure 7 - 8 and Table 1 also revealed five subsurface geoelectric units for VES 16 and 18 and four layers in VES 17, 19 and 20, the topsoil (sandy-clay) of thickness and resistivity values ranging from 0.286 - 2.000 m and 53.330 - 3419.500 Ωm respectively. The topsoil was underlain by a less resistive layer except in VES 19 and had resistivity and thickness values

ranging from 530.900 - 3963.900 Ωm and 3.260 - 6.020 m respectively. The third layer which was the aquifer layer of VES 17, 19 and 20 had thickness and resistivity values of 14.030 - 47.530 m and 153.100 - 1915.800 Ωm . The fourth layer with higher resistivity value in VES 18 than 16 was characterized as the aquifer zone of the VES points which exhibited a higher groundwater potential as shown by VES 18.

Vertical soundings conducted as VES 21, 22, 23, 24 and 25, shown in figure 9 - 10, revealed a four-layer earth in VES 21, 22 and 25 and three layer for VES 23 and 24. The topsoil (sandy-clay) layer of the VES points exhibited thickness and resistivity values ranging from 0.220 - 2.020 m and 440.300 - 1764.300 Ωm and it was underlain by an aquifer layer shown in VES 23 and 24, the layer possessed resistivity and thickness values ranging of 213.600 - 2878.800 Ωm and 2.850 - 16.940 m. The third geoelectric unit of VES 21, 22 and 25 was the water bearing unit (aquifer) of the VES points which had resistivity and thickness values ranging from 617.400 - 6463.500 Ωm and 11.080 - 21.380 m and the aquifer layers were inferred as sandstone. The presence of a very low resistivity geoelectric unit overlain by aquifer in VES 22 and VES 25 locations signified the existence of an unconfined aquifer which affects the groundwater potential of the study area seasonally.

THICKNESS OF THE AQUIFER ZONES

In this research, 2D contour map illustrating the aquifer thickness within the study region was produced (Figure 11). North-western and South-western part of the study area has shown high value of groundwater potential due to their high aquifer thickness value which was low in other part. VES 1, 2, 3, 4 and 5 carried out in Guduma ward with an electrode spacing of 200 m has showcased a higher potential for groundwater exploration than other VES locations conducted in the area and VES 4 had the highest potential with thickness value of 80.760 m and VES 23 conducted in Namne ward possessed the lowest groundwater potential with thickness value of 2.850 m. The greater thicknesses observed in study area indicate higher storage capacity for groundwater, which implies a greater potential for groundwater extraction. These findings bear significant implications for groundwater resource management, as areas with thicker aquifers may offer favorable conditions for sustainable extraction practices.

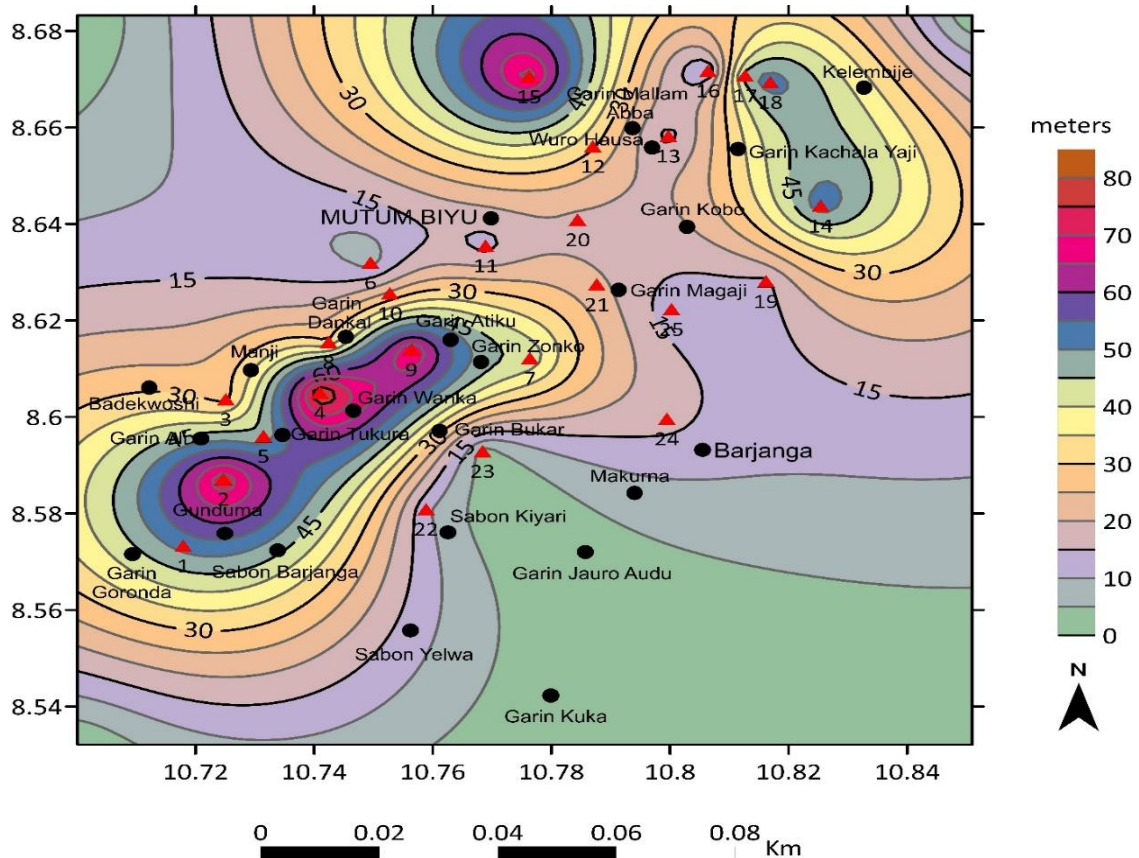


Figure 11: Aquifer thickness map of study area

DEPTH TO AQUIFERS ZONES

The aquifer depth represents the vertical distance between the saturation zone and the overlying zones of aeration, situated above the water table. During rainfall events, water infiltrates through void/fractures in the soil and rock, descending under the influence of gravity. Consequently, water accumulates and fills the lower region, known as the zone of saturation. To visualize the spatial distribution of aquifer depth within the research area, Figure 12 presents a 2-D contour map. Among the VES locations, VES 23 exhibited the shallowest depth, measuring 3.300 m, while VES 4 represented the deepest with an aquifer depth of 93.700 m. These variations in aquifer depth highlighted the heterogeneity of earth crust.

Understanding aquifer depth is critical for assessing groundwater availability, evaluating the vulnerability of the aquifer system, and devising effective management strategies. Shallow aquifer depths may indicate areas more susceptible

to fluctuations in water table levels and have implications for sustainable groundwater utilization as witness in Gassol.

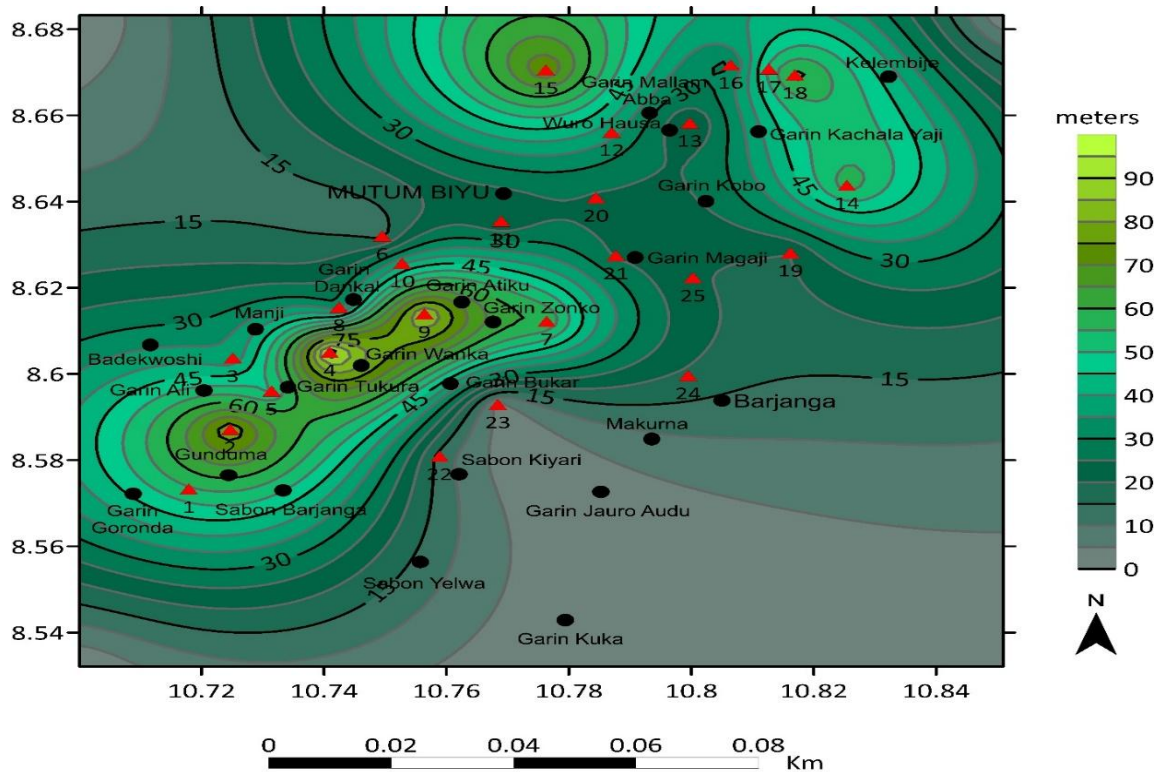


Figure 12: Aquifer depth map of the study area

GEOELECTRIC SECTION

The geoelectric parameters of some resistivity sounding (selected based on proximity and linearity) were used to construct model of the geoelectric sections of the study area. The importance of geoelectric sections is to map the variations of geoelectrical parameters along a linear path (Adagunodo *et al.* 2017; Sunmonu *et al.*, 2015; Raji and Adeoye, 2017). Five traverses were drawn along the VES location: traverse 1(T1) of along VES 1 and VES 2, in NE-SW direction, T2 of along VES 7 and VES 10 in NW-SE direction, T3 along VES 21 and VES 24, in NW-SE direction, T4 along VES 19 and 20, in NW-SE direction, and T5 of along VES 13 and VES 14 in NW-SE direction. The geoelectric sections of the five traverse in the different wards in NE-SW orientation of the study area, as shown in figure 13-17 were plotted in order to map the depth to the aquifer layers and this revealed an increase in aquifer depth towards NE along T1 with VES 2 having more depth than VES 1, towards SE along T2, towards SE along T3, towards SE along T4 and towards SE along T5. The depth

to aquifer layer along these traverses varies due to the existence of an unconfined aquifer at varying VES points and this is in line with the groundwater flow direction of the area.

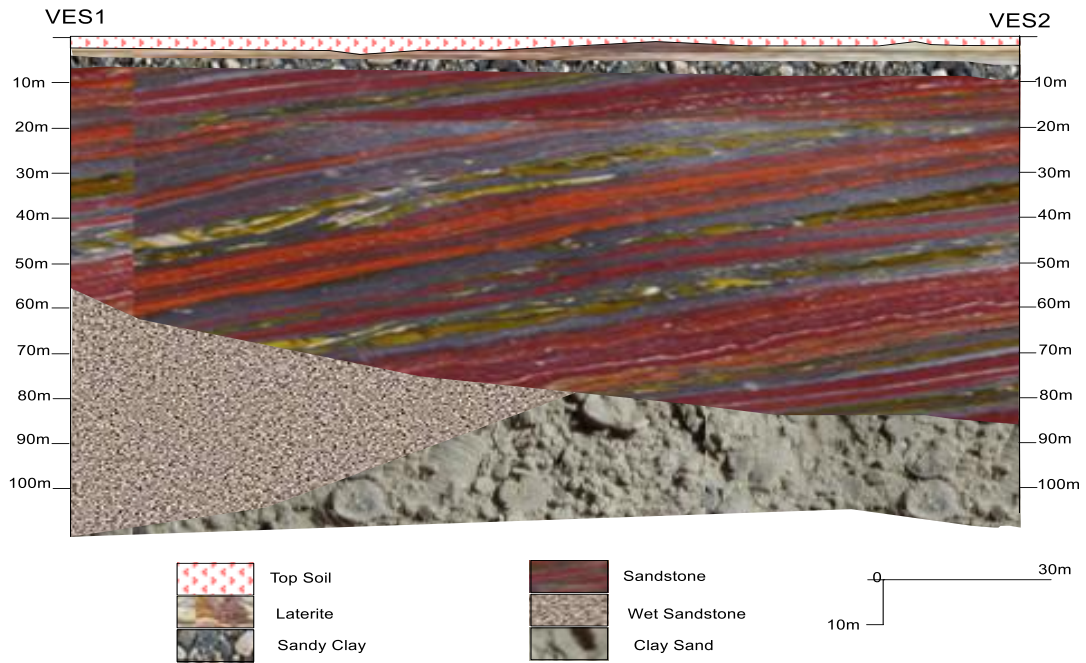


Figure 13: Goelectric Section of T1 along VES 1 and VES 2

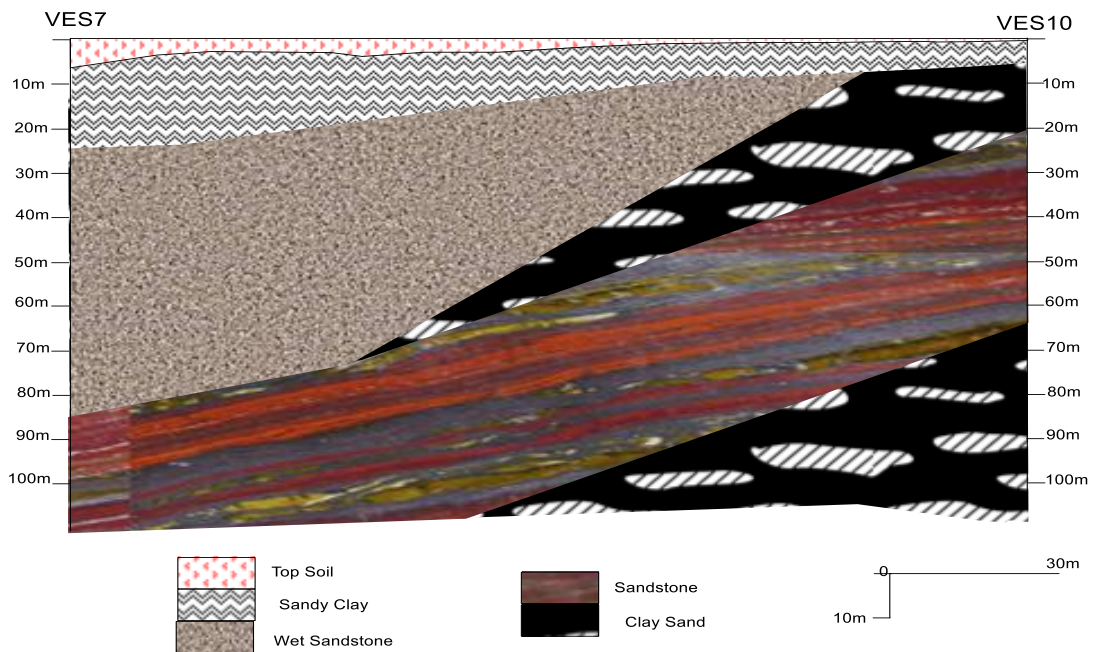


Figure 14: Goelectric Section of T2 along of VES 7 and VES 10



Figure 15: Goelectric Section of T3 along VES 21 and VES 24

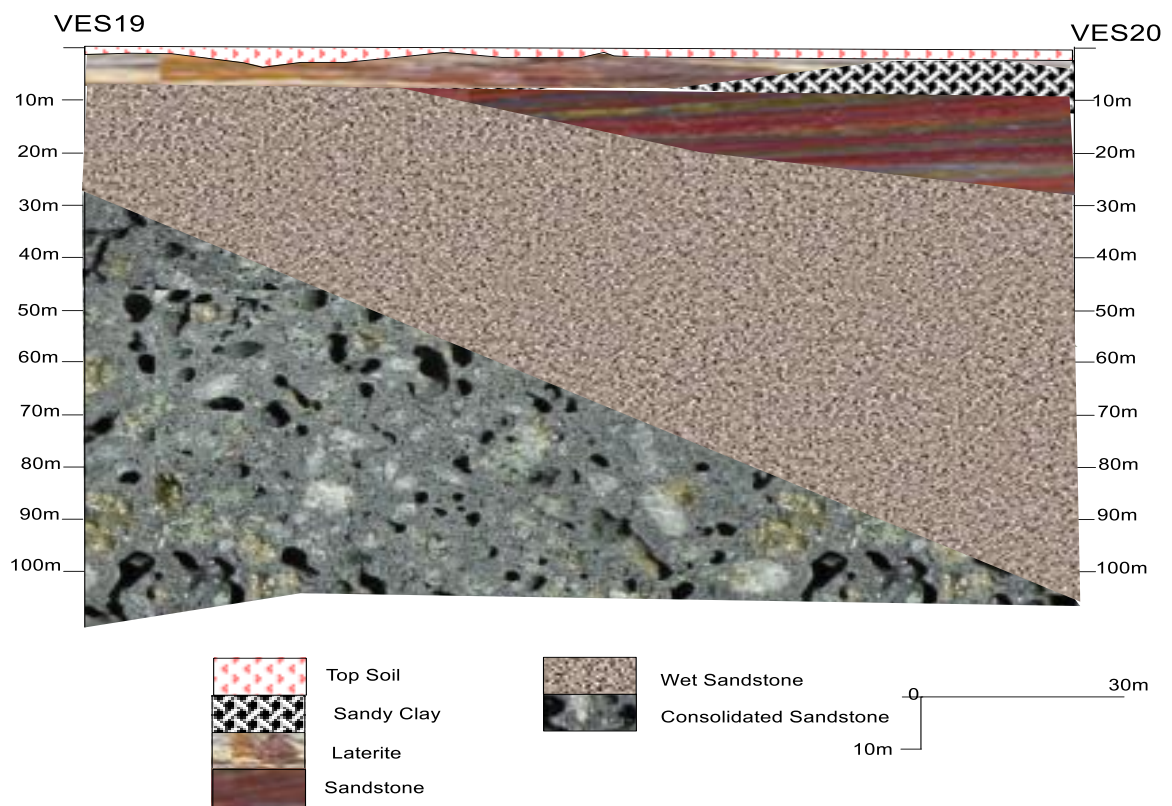


Figure 16: Goelectric Section of T4 along VES 19 and VES 20

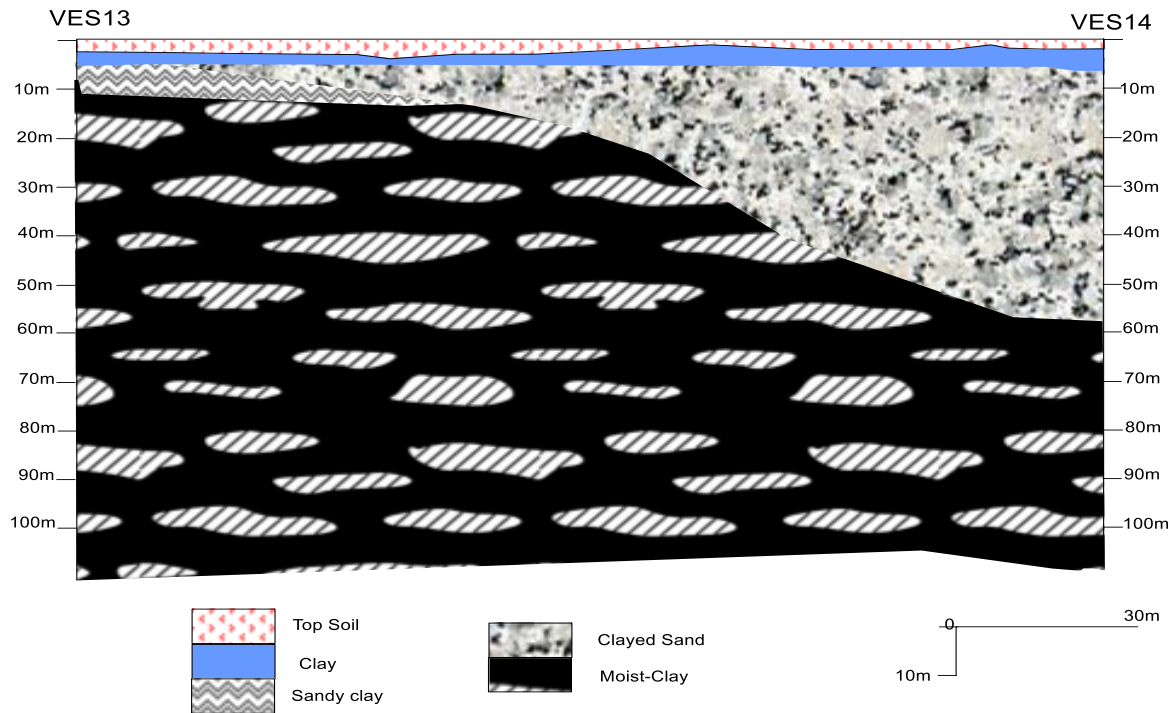


Figure 17: Geoelectric Section of T5 along VES 13 and VES 14

T1 in NE-SW direction showed that aquifer zone may be reached at depth of 54.300 m for VES 1 and 79.650 m for VES 2 which shows an increase in the aquifer depth towards the NE direction respectively. T2 revealed that the aquifer depth in NW-SE orientation is 59.870 m for VES 7 and 39.650 m for VES 10 respectively. T3 in the NW-SE direction further revealed that depth to aquifer strata towards the NW part of the study area is higher than towards SE. T4 in the NW-SE direction unfolds an increase in aquifer depth towards the NW orientation that ranged between 20.050 m and 24.330 m and T5 along VES 13 and VES 14 shows depth of aquifer ranging between 19.620 m and 57.680 m with a deep aquifer depth observed at VES 14 respectively.

CONCLUSION

The results of the geophysical investigation conducted Gassol L.G.A in order to evaluate the seasonal variation/change in groundwater potential of the area. The result revealed a five geoelectric layers with shallow aquifer depth of less than 50 m in most VES points except in VES 1, 2, 4, 9, 14, 15, 17 and 18, due to the hydrogeological condition of the study area higher aquifer depth was expected and

also lower resistivity layer overlain by the aquifer was revealed which showed the existence of an unconfined aquifer and this is seen in VES 2, 9, 10, 11, 12, 14, 16, 22, and 25 and its the hydrogeological caused of the seasonal variation/change in the groundwater potential. Successful groundwater exploration and extraction in the study area required deeper geophysical resistivity survey involving wider electrodes spacing greater than 200 m to reach the confined aquifer. The results also from the evaluated geoelectric parameters (resistivity and thickness) showed that the area has high groundwater potential.

REFERENCES

1. Adagunodo, T. A., Adeniji, A. A., Erinle, A. V., Akinwumi, S. A., Adewoyi, O. O., Joel, E. S., and Kayode, O. T. (2017). Geophysical Investigation into the Integrity of a Reclaimed Open Dumpsite for Civil Engineering Purpose. *Inter. J.* 42(11), 324-339.
2. Adeniji, A. E., Obiora, D. N., Omonona, O. V. and Ayuba, R. (2013). Geoelectrical Evaluation of Groundwater Potentials of Bwari Basement Area, Central Nigeria. *Int J PhysSci*, 8(25):1350-1361. <https://doi.org/10.5897/IJPS2013.3951>
3. Adeniji, A., Omonona, O., Obiora, D., and Chukudebelu, J. (2014). Evaluation of Soil Corrosivity and Aquifer Protective Capacity using Geoelectrical Investigation in Bwari Basement Complex area, Abuja. *Journal of Earth System Science*, 123, 491-502.
4. Adeyolanu, O. D., Are, K. S., Adelana, A. O., Denton, A. O., Oluwatosin, G. A., Ande, O. T., Ojo, A. O. and Adediran, J. A. (2020). Assessing Quality of Rice Producing Soils Using Two Methods of Quantification. *European Journal of Agriculture and Forestry Research*, vol.8(3), pp.1-16.
5. Akinwumiju, A. S., Olorunfemi, M. O., and Afolabi, O., (2016): GIS Based Integrated Groundwater Potential Assessment of Osun Drainage Basin, Southwestern Nigeria. *Ife J. Sci.*, 18(1), 147–168. <https://www.ajol.info/index.php/ij/article/view/148348>

6. Cobbina, S. J., Nsonwah, E., Duwiejuah, A. B., and Nkoom, M. (2014). Assessment of Trace Metals in Soil At The Bulk Oil Storage And Transportation (BOST) Facility In Buipe, Ghana. *Res. J. Chem. Environ. Sci.*, 2, 40–47,
7. Egbai, J. C. (2013). Aquifer Comparability and Formation Strata in Orogun And Osubi (Ugolo) Area of Delta State using Electrical Resistivity Method, *Int. J. Res. Rev. Appl. Sci.* 14 682–691.
8. El-Osta, M., Masoud, M., and Badran, O. (2021) Aquifer Hydraulic Parameters Estimation Based on Hydrogeophysical Methods in West Nile Delta. *Egypt Environ Earth Sci.*; 80:1–17.
9. Joel, E. S., Peter, I. O., Theophilus, A.A., Maxwell, O., Ifeanyi, O., Marvel L. A. and Olukunle, C. O. (2020). Geo-Investigation on Groundwater Control in Some Parts of Ogun State Using Data from Shuttle Radar Topography Mission and Vertical Electrical Soundings, *Heliyon* vol.6 <https://doi.org/10.1016/j.heliyon.2020.e03327>
10. Mark, A., Amadi, A. N., Christopher, U., Jude, S. E. (2000). Hydrogeophysical Investigation of Groundwater Systems in Otukpo, Benue State, North-Central Nigeria, *J. Chem. Soc. Nigeria*, Vol. 45, No.5, Pp 897 – 905.
11. National Population Commission (2006). Population and Housing Census of the Federal Republic of Nigeria 2006 Census: Priority Tables, Abuja, Nigeria.
12. Nwachukwu, S. R., Bello, R., Ayomide, O., Balogun, A. O. (2019). Evaluation of Groundwater Potentials of Orogun, South–South Part of Nigeria Using Electrical Resistivity Method. *Applied Water Science*, 9: 184. <https://doi.org/10.1007/S13201-019-1072-Z>
13. Oladunjoye, M. and Jekayinfa, S. (2015). Efficacy of Hummel (Modified Schlumberger) Arrays of Vertical Electrical Sounding in Groundwater Exploration: case study of parts of Ibadan Metropolis, Southwestern Nigeria. *J Geophys.* <https://doi.org/10.1155/2015/612303>.

14. Oliver, S. G. H., John, C. and Ingrid, C., (2006) Protecting Groundwater for Health Managing the Quality of Drinking-water Sources. London: IWA Publishing, Alliance House.
15. Olorunfemi, M. O., Ojo, J. S., Idornigie, A. I., and Oyetoran, W. E. (2005). Geophysical Investigation of Structural Failure of a Factory Site in Asaba area, southern Nigeria. *J Min Geol* 41(1): Pp.111-121.
16. Owolabi, A., Charles, I. K. and Patience, O. S. (2022). Groundwater Potential Assessment of the Sedimentary and Basement Complex Rocks of Ogun State, Southwest Nigeria. *Journal of Water and Environment Technology*. Vol. 20(6), Pp. 248-260, Doi:10.2965/Jwet.21-177
17. Raji, W. O., and Adeoye, T. O. (2017). Geophysical mapping of contaminant leachate around a reclaimed open dumpsite, *J. king saud. Univ. sci.* 29, 348-359.
18. Sunmonu, L. A., Adagunodo, T. A., Adniji, A. A., Oladejo, O. P., Alagbe, O. A. (2015). Geophysical Delineation of Aquifer Pattern in Crystalline Bedrock. *Open Trans. Geosci.* 2(1), 1-16.
19. Talabi, A. O. (2018). Estimated Volume of Water in Shallow Wells of Ekiti State, Southwestern Nigeria: Implications on Groundwater Sustainability. *Arab. J. Geosci.*, 11(21), 681. <https://doi.org/10.1007/s12517-018-4031-3>